UPSTREAM FIELD-ALIGNED BEAMS: RESULTS FROM CLUSTER

Meziane, K.[(1)], Wilber, W.[(2)], Hamza, A. M.[(1)], Mazelle, C.[(3)], Parks, G. K.[(2)], and Rème, H.[(3)]

[(1)] University of New- Brunswick, Fredericton, Canada (karim@unb.ca).
[(2)] University of California, Berkeley, USA.
[(3)] Centre d'Etude Spatiale des Rayonnements, Toulouse, France.

ABSTRACT

Cluster observations on field-aligned beams (FABs) upstream of the bow shock are presented. They include both single and multispacecraft data in the analysis. We will emphasis new features that have not been reported previously. When these field-aligned beams are observed, the ULF waves are not present. Detailed examination of reduced distribution functions indicates the existence of a high energy tail associated with ion beams having significant non-zero pitch-angle values. We found that the tail progressively develops when the angle θ_{Bn} between the ambient IMF and the local shock normal decreases from quasi-perpendicular to oblique shocks. Also, Cluster reveals the existence of a very sharp boundary separating the FABs from gyrating ion populations in the foreshock, possibly indicating a shock geometry threshold where the FABs production mechanism breaks down or a competing mechanism dominates. We found that the properties of protons propagating along this boundary do not agree with any known emission mechanisms at the shock. We will discuss some physical hypothesis which might be able to explain these new results.

1. INTRODUCTION

Broad classes of upstream ions propagating sunward are commonly observed when the interplanetary field lines are connected to the Earth's bow shock. Several types of upstream ion distributions in the Earth's foreshock have been identified and extensively studied in the past twenty five years [1][2]. The differing ion types statistically have a dependence upon the shock geometry, which is dtermined by the angle θ_{Bn} that the local shock normal makes with the magnetic field direction. Within quasi-parallel regions ($\theta_{Bn} \leq 45^{O}$) we typically see diffuse populations, which consist of nearly isotropic shell distributions with thermal energies of a few tens to ~ 300 keV. Oblique shock regions contain intermediate and gyrating distributions. The former appear field-aligned, but have a large spread in pitch angles. The latter have phase space density peaks at non-zero pitch-angle and may appear gyrotopic or not (gyrophased bunched). These three types of distributions are all observed in association with large amplitude ($\delta B/B \sim 1$) ultra-low frequency (ULF) magnetohydrodynamic waves. Field-aligned beams (FABs), which consist of ions collimated along the interplanetary magnetic field, are usually found within quasi-perpendicular regions ($45^{o} \leq \theta_{Bn} \leq 70^{o}$). They energy may extend up to ~ 20 keV and they are never observed in association with ULF waves. In the present paper, our interest is with field-aligned beams.

Although significant investigations have been carried out in the previous years, the detailed dymanics producing the FAB distributions at the shock is poorly understood. The simplest kinematic descriptions of reflection, based or not upon the invariance of the magnetic moment μ, fail to account for the large increase in thermal energies of the backstreaming ion populations relatively to that of the solar wind. Understanding the production mechanism responsible for coherent distribution functions is of fundamental importance in shock acceleration. The recent high quality data obtained from Cluster allow for detailed quantitative studies and the deconvolution of spatial and temporal variations. We examine in this paper, some new observations from Cluster-CIS experiment.

2. INSTRUMENTATION

The particle data used in this study are from Cluster Ion Spectrometer experiment which includes i)- a Hot Ion Analyser (HIA) which measures particles in the energy range 0.005-26 keV; ii)- a time-of-flight mass spectrometer (CODIF), which combines a top-hat analyser with a time-of-flight section to measure the major species: H+, He+, He++ and O+. The sensor primarily covers the energy rangle between 0.02 keV/q and 38 keV/q. Both instruments measure full 3D distributions within one satellite spin period (4~sec) with an angular resolution of 22.5° x 22.5°. In normal telemetry mode, one distribution is transmitted every 2 spins (or 3 spins depending on the time period), whereas in burst mode the distribution is transmitted every one spin. A detailed description of the Cluster-CIS experiment can be found in the work of [2]. With the above instrumental characteristics both the solar wind plasma as well as the energetic particles are detected. The HIA analyser operates with high geometry factor (HIA-G) appropriate for upstream ions measurement as well as with low geometry factor (HIA-g) for the solar wind plasma measurement.
Our study also uses magnetic field data which come

from the fluxgate magnetometer (FGM) installed on board the Cluster spacecraft [3]. We have used 4s-time resolution averaged magnetic field components to investigate the association of low-frequency waves with the backstreaming ions.

3. BEAM PROPERTIES

We present in this section field-aligned beam observations when changes in the angle θ_{Bn} (i.e. slow IMF rotation), whereas the location of the spacecraft is essentially fixed. Figure 1 shows exemple of 2D ion distributions from Cluster SC1 measured on April 23, 2001. The distributions are sampled in the solar wind frame of reference. The snapshots have been presented sequentially to show the variation in time of the distributions.

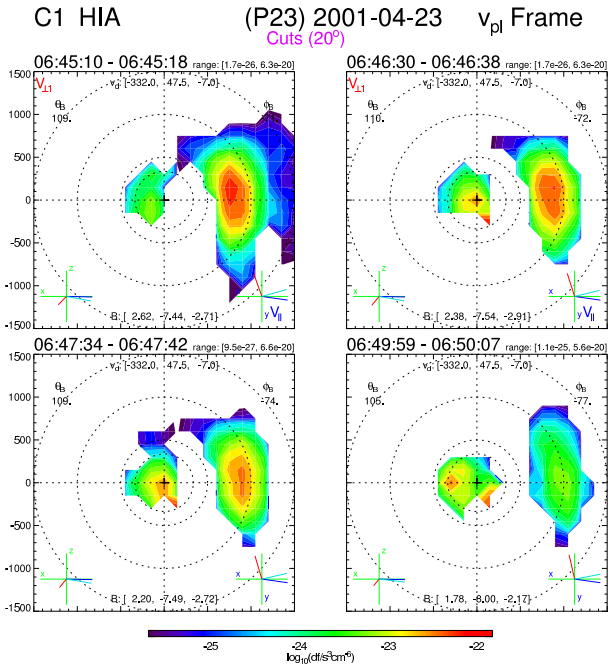

Figure 1. Ion distribution functions from Cluster SC1 CIS/HIA, April 23, 2001, 0645:10-0650:07 UT.

Clearly, Figure 1 indicates the particle distributions correspond to beams collimated along the magnetic field direction; it also shows that beam parallel velocity increase as a function of time. We mention that the component of the distribution near to the origin corresponds to the solar wind. In order to establish relationships between the FABs and the shock geometry, the moments of the distributions have been carefully determined. The shock geometry (θ_{Bn} and θ_{Vn}) is determined by projecting the IMF line crossing the spacecraft to a widely-used statitistical bow shock model such as of Cairns et al. [5]. Figure 2 shows moments computed for successive FABs observed on April 23 2001, 0647-0651 UT. These moments are plotted versus θ_{Bn} angle.

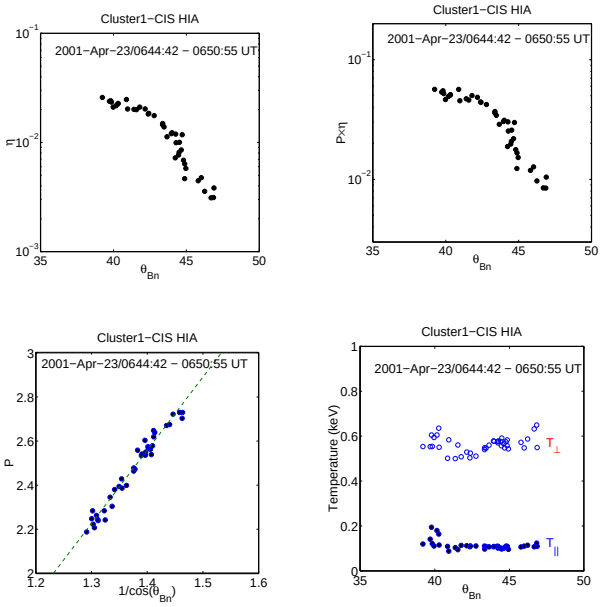

Figure 2. Upstream moments versus θ_{Bn} angle. Normalized density (top left panel), normalized particle flux (top right panel), normalized parallel beam speed (bottom left panel), beam temperatures $T_{\parallel}$ and $T_{\perp}$ (bottom right panel).

Figure 2 shows good correlation between the shock geometry and the FAB moments. The decrease in beam density (normalized to the solar wind density) η is expected since only particles moving upstream in the deHoffman-Teller frame will escape upstream. The θ_{Bn} increase requires that the particles originate from further in the tail of the distribution. A plateau-like in density seen for low θ_{Bn} values inidicates that the beam production mechanism beaks down for a certain critical θ_{Bn}. Density values as low as 10^{-4} as seen here, may lead, in an ion-ion cyclotron instability, to an *e*-folding growth times in order of ~200s, which leads to a total distance of ~30R_E before significant disruption. Similar correlation with θ_{Bn} angle is observed for the beam production efficiency $P\times\eta$. This strong variation provides an important constraint on any dynamical models for the FABs production. For exemple, we note that the observed production efficiency is opposite to the upstream escape model reported by Tanaka et al. [6].
Figure 2 also shows a clear linear dependence of the normalized beam speed P (= v_B/v_{SW}) upon $1/\cos\theta_{Bn}$. The $1/\cos\theta_{Bn}$ factor appears in the expression for the deHoffman-Teller frame speed V_S writen in the solar wind frame of reference. According to the kinematical

description of ion reflection by Sonnerup [7], the upstream beam normalized speed is $P \sim (1+\delta)/\cos\theta_{Bn}$. where $\delta \sim 1$ for an adiabatic reflection and $\delta \neq 1$ otherwise. For FABs presented in Figure 2, we have found $\delta \sim 2$.

Finally, the FAB temperatures $T_{\|}$ and $T_{\perp}$ are shown on Figure 2. A temperature anisotropy of ~5 is observed, which is consistent with presvious results. Most notable is that there is no clear dependence of either temperatures upon θ_{Bn}. A straight free escape condition for particles in a source distribution at the shock would lead a strong dependence of $T_{\perp}$ upon θ_{Bn}.

4. AN INNER BOUNDARY

The different classes of populations observed upstream are observed in distinct regions in the foreshock. FABs are seen in a layer 0f ~ 0.4 R_E thickness, followed downstream by a ~ 3.5 R_E- wide layer of intermediate ions [8]. Gyrophase- bunched ions are likely present in a thin region at the edge of the FABs region. A spatial bounadry between population is therefore expected since the simultaneous observations of two different types of population has never been reported previously. However, a spatial foreshock boundary separating regions where ULF waves are present from those where they are absent has been reported [9]. Subsquently, Le & Russell [10] found a similar boundary, but its geometrical characteristics differ significantly.

Recently, a sharp spatial boundary separating FABs and gyrophase- bunched ions have been found using CLUSTER- CIS data [11]. Figure 3 shows successive spectra from CIS/CODIF experiment on SC1; it indicates an apparent and progressive merging of an energetic population (secondary peak) with FABs (primary peak). Detailed examination of the three- dimensional distribution functions indicated that the energetic component is a remote- sensed gyrophase- bunched ion population. Figure 4 illustrates the remote sensing model accounting for the two- peak spectra. The particles travelling along the field line threading the spacecraft S correspond to the main peak in Figure 3. Simultaneously, the spacecraft detects gyrating ions at high energy having guiding centers along adjacent field lines separated by less than one gyroperiod. Only particles having a suffisant energy may be detected at S. The existence of the spatial boundary found here indicates that the transition between FABs and gyrophase- bunched ion population occurs within ~ 1 gyroradius. We have found that this boundary agrees with the ULF wave boundary found previously by Le and Russell [10] and the one predicted theoretically [12]. Finally, it is worth to mention that the FABs travelling along this boundary do not match any known shock emission mechanism.

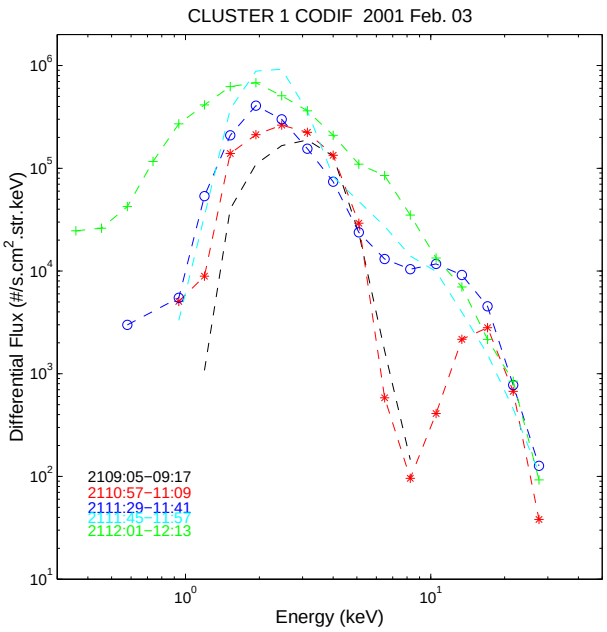

Figure 3. Spectra from CLUSTER SC1 CIS/CODIF for successive times registered on 2001 Feb. 03.

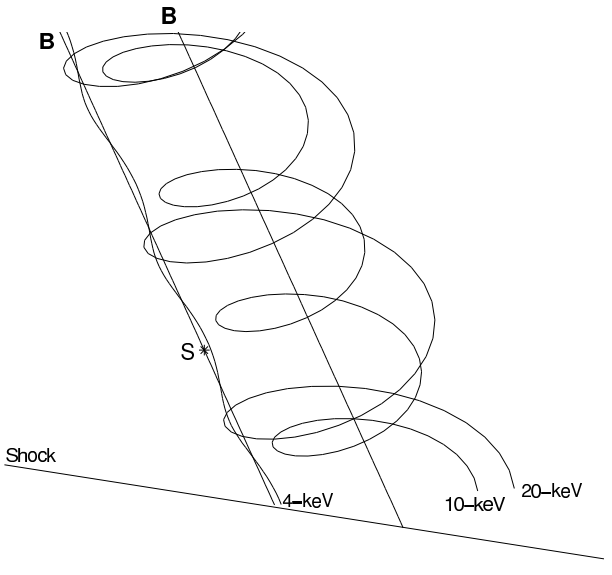

Figure 4. Schematics showing how large particle gyroradii are remotely detected by the spacecraft (S).

5. REDUCED DISTRIBUTION FUNCTIONS

In this section we present an example of reduced distribution functions $f(v_{\|})$ and $f(v_{\perp})$ associated with FABs. Figure 5 shows reduced distribution functions observed simultaneously by spacecraft SC1 and SC3 on January 28, 2003.

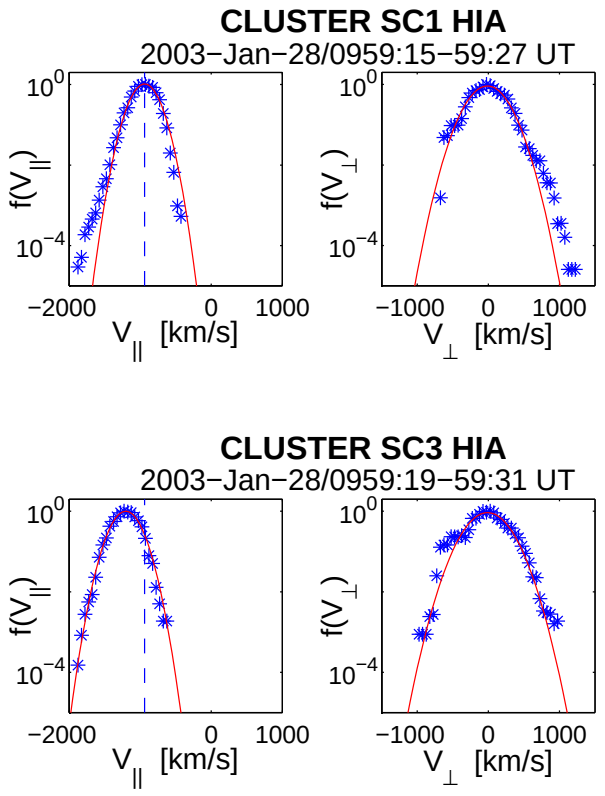

Figure 5. Reduced distributions function $f(v_{||})$ and $f(v_{\perp})$ on January 28, 2001 registered by CIS-HIA experiemnt onbord SC1 (top panels) and SC3 (bottom panels).

The two spacecrafts were separated by ~ $1R_E$, and the spacecraft SC1 was located downstream from SC3. For clarity, in each panel the red curve indicates the best fits to Maxwellians. These fits seems satisfactory for the FAB observed at SC3, whereas the FAB observed by SC1 exhibits a high energy tail. It is important to mention, that the Maxwellian beam has a higher speed (v^{SC3} = 1200 km/s against v^{SC1} = 935 km/s). We have demonstrated on other events not shown here that as θ_{Bn} decreases, the high energy tails appear extending to lower energies. Also, the non-thermal parts of these ion distributions are not field-aligned. Up to now, there is no satisfactory explanation for the prodection of theses high energy tail.

6. CONCLUSION

The fundamental questions about the underlying mechanisms producing the field-aligned beams have not yet received satisfactory answers. Models based upon the guiding center approximation and those which introduce diffusion as a mean of enhancing the fluxes of upstream beams fail to produce the properties observed.

ACKNOWLEDGMENTS

We thank the International Space Institute (ISSI) in Bern for their support of this work, and members of the ISSI Upstream Ions Collaboration for useful discussions. Work at UNB is supported by the Canadian Natural Science and Engineering Council.

REFERENCES

1. Thomsen, M. F., *Upstream Suprathermal Ions*, in Collisionless Shocks in the Heliosphere: A tutorial Review, edited by R. G. Stone and B. T. Tsurutani, AGU, Geophysical Monograph 35, 253-270, 1985.

2. Fuselier, S. A., *Suprathermal ions upstream and downstream from the Earth's bow shock, in Solar Wind Sources of Magnetospheric Ultra-Low Frequency Waves*, edited by Engebretson, M. and Takahashi, M. and Scholer, M., AGU, Geophysical Monograph 81, 91-114, 1994.

3. Rème, H. et al., *First multispacecraft ion measurements in and near the Earth's magnetosphere with identical Cluster ion spectrometry (CIS) experiment*, Ann. Geophysicae, Vol. 19, 1303-1354, 2001.

4. Balogh, A., *The Cluster magnetic field investigation: overview of in-flight performance and initial results*, Ann. Geophysicae, Vol. 19, 1207-1217, 2001.

5. Cairns, I. H., D. H. Fairfield, R. R. Anderson, V. E. H. Carlton, K. I. Paularena, and A. J. Lazarus, *Unusual location of Earth's bow shock on September 24-25, 1997: Mach number effects*, Journal of Geophysical Reserch, Vol. 100, 47-62, 1995.

6. Tanaka, M., C. C. Goodrich, D. Winske, and K. Papadopoulous, *A source of the backstreaming ion beams in the foreshock region*, Journal of Geophysical Research, Vol. 88, 3046-3054, 1983.

7. Sonnerup, B. U. O., *Acceleration of particles reflected at a shock front*, Journal of Geophysical Research, Vol. 74, 1301-1304, 1969.

8. Bonifazi, C., and G. Moreno, *Reflected and diffuse ions backstreaming from the Earth's bow shock, 1. Basic properties*, Journal of Geophysical Research, Vol. 86, 4381-4396, 1981.

9. Greenstadt, E. W., and L. W. Baum, *Earth's compressional foreshock boundary revisited: observations by the ISSE-1 magnetometer*, Journal of Geophysical Research, Vol. 91, 901-, 1986.

10. Le, G. and C. T. Russell, *A study of ULF wave foreshock morphology, 1. ULF foreshock boundary*, Planetary and Space Science, Vol. 40, 1203-1213, 1992.

11. Meziane, K. et al., *Simultaneous observations of field-aligned beams and gyrating ions in the terrestrial foreshock*, Journal of Geophysical Research, Vol. 109, doi: 10.1029/2003JA010374, 2004.

12. Skadron, G. R., R. T. Holdaway, and M. A. Lee, *Formation of the wave compressional boundary in the Earth's foreshock*, Journal of Geophysical Research, Vol. 93, 11354-11362, 1988.